Electronic supplementary information

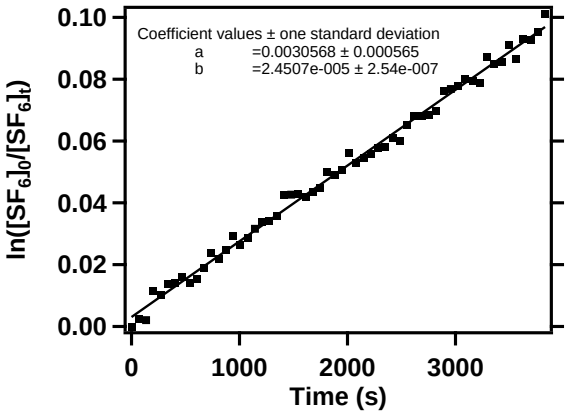

Figure S1 The first order decay rate of SF_6 in the chamber

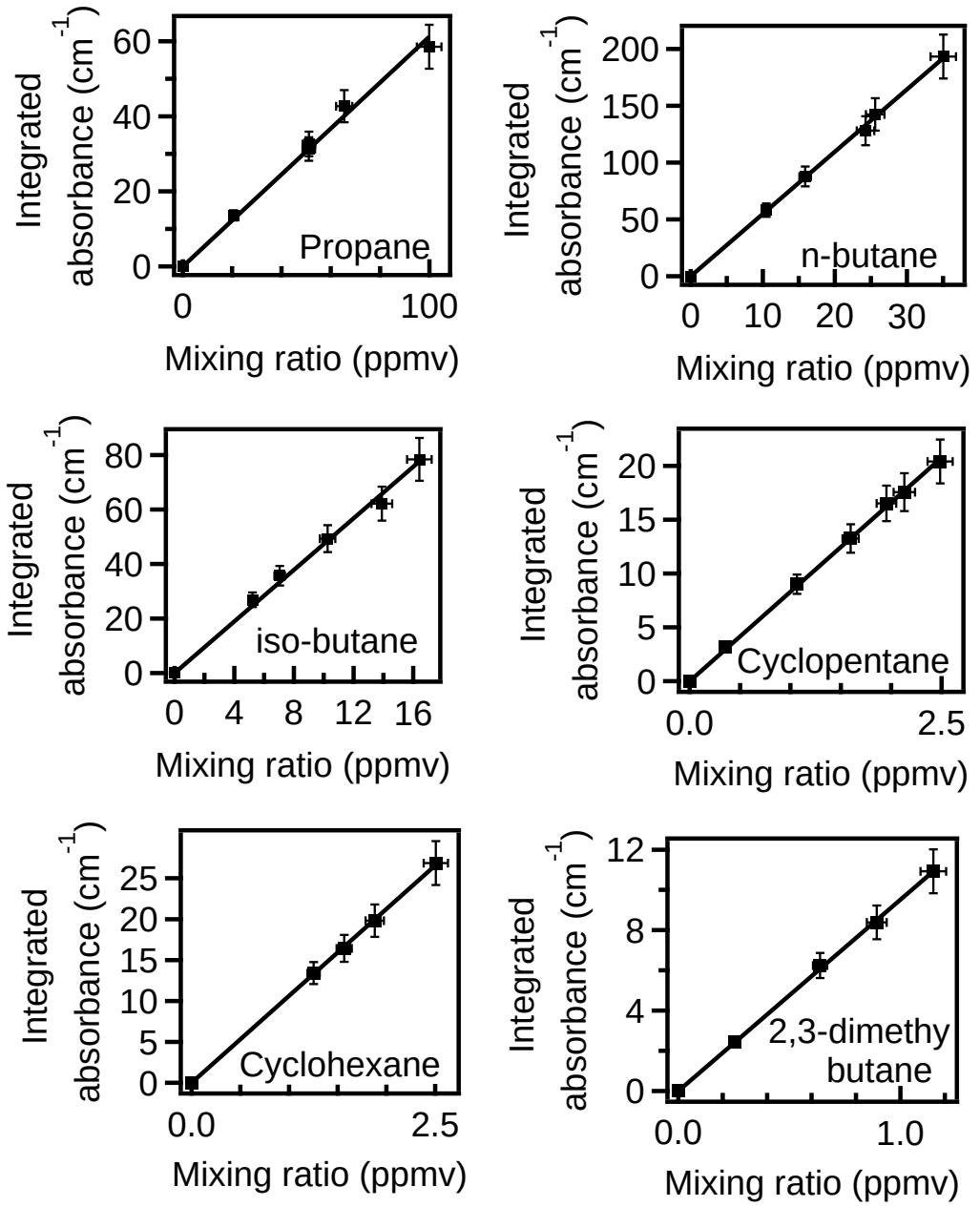

Figure S2 Calibration curve for each alkane from FTIR by plotting the integrated absorbance against known mixing ratio of the hydrocarbon (ppmv).

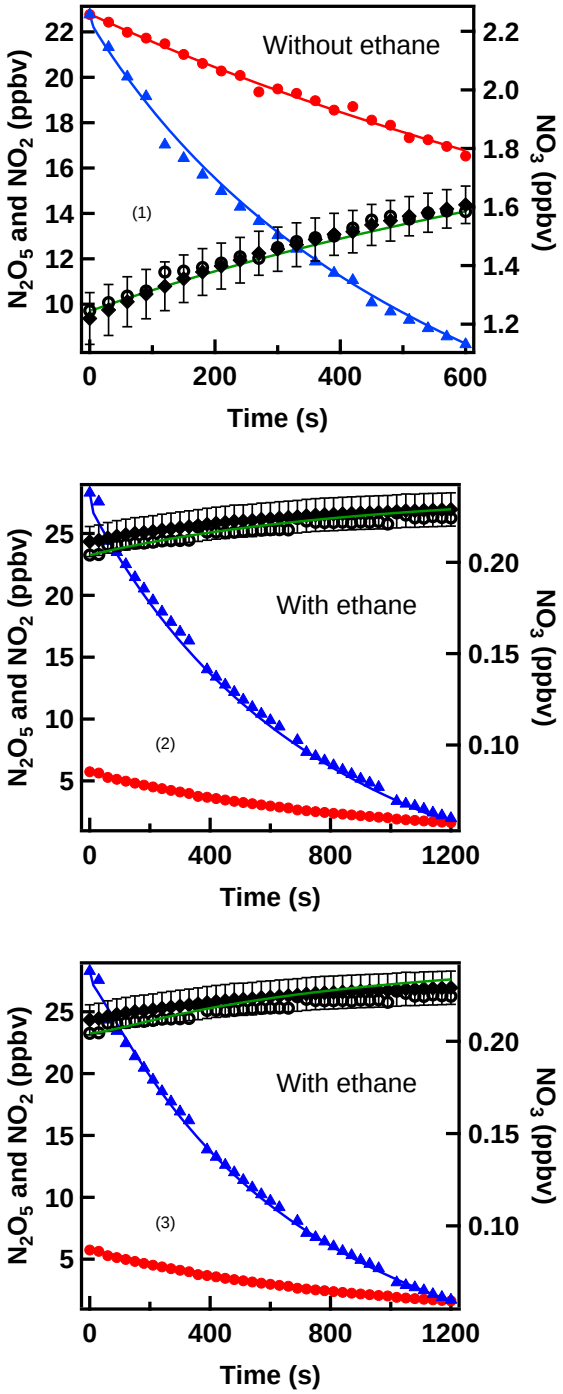

Figure S3. Experimental and simulated NO_3, N_2O_5 and NO_2 concentration profiles versus reaction time. Measured NO_3 (▲), N_2O_5 (●) and NO_2 (◆) are shown along with their simulated temporal profiles (—NO_3, —N_2O_5, —NO_2). Also shown is NO_2 concentration calculated from the Keq and the observed of N_2O_5 and NO_3 concentrations (O). Top panel: 0 ppmv C_2H_6. Middle panel: 1106 ppmv C_2H_6 and secondary reactions not included, yields a value of $k_2 = 7.60 \times 10^{-19}$ molecule^{-1} cm^3 s^{-1}. Bottom panel: 1106 ppmv C_2H_6 with secondary reactions included (see Table 1), yields a value of $k_2 = 4.23 \times 10^{-19}$ molecule^{-1} cm^3 s^{-1}.

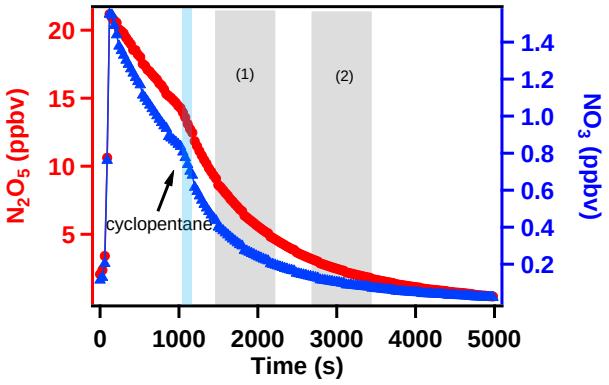

Figure S4 NO_3 and N_2O_5 profiles from chamber experiment cyclopentane reacting with NO_3 radicals (The blue bar indicates the time at which cyclopentane was injected into the chamber and the time it took for complete mixing.). Two separate reaction periods are noted in the figure. Fitting the observed profile within these two periods yielded the same value for the rate coefficient.

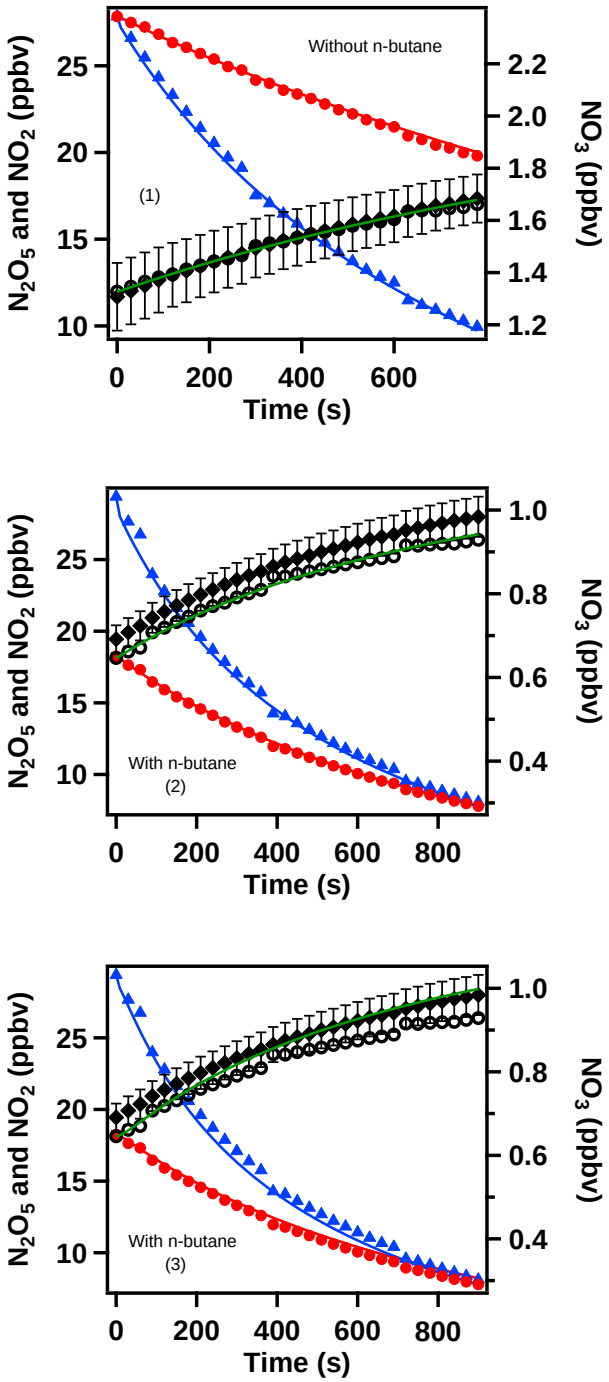

Figure S5. Experimental and simulated NO_3, N_2O_5 and NO_2 concentration profiles versus reaction time. Measured NO_3 (▲), N_2O_5 (●) and NO_2 (◆) are shown along with their simulated temporal profiles (—NO_3, —N_2O_5, —NO_2). Also shown is NO_2 concentration calculated from the Keq and the observed of N_2O_5 and NO_3 concentrations (O). Top panel: 0 ppmv n-C_4H_{10}. Middle panel: 19.72 ppmv n-C_4H_{10} and secondary reactions not included, yields a value of $k_4 = 3.10 \times 10^{-17}$ molecule^{-1} cm^3 s^{-1}. Bottom panel: 19.72 ppmv n-C_4H_{10} with secondary reactions included (see Table 1), yields a value of $k_4 = 1.35 \times 10^{-17}$ molecule^{-1} cm^3 s^{-1}.

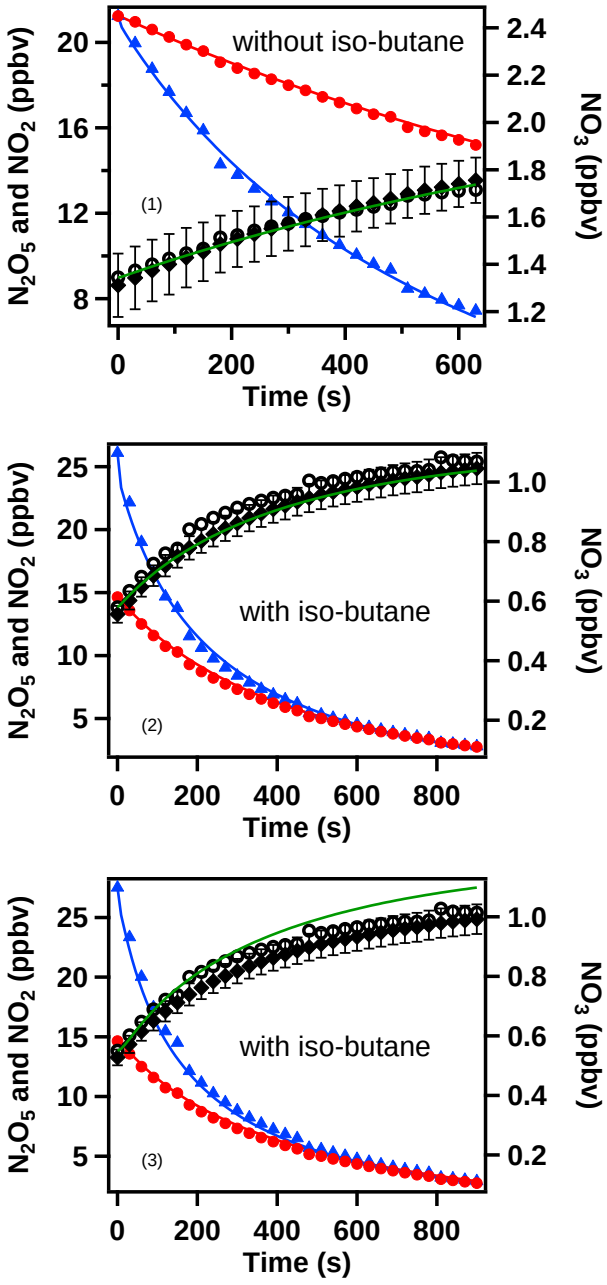

Figure S6. Experimental and simulated NO_3, N_2O_5 and NO_2 concentration profiles versus reaction time. Measured NO_3 (▲), N_2O_5 (●) and NO_2 (◆) are shown along with their simulated temporal profiles (—NO_3, —N_2O_5, —NO_2). Also shown is NO_2 concentration calculated from the Keq and the observed of N_2O_5 and NO_3 concentrations (O). Top panel: 0 ppmv iso-C_4H_{10}. Middle panel: 19.72 ppmv iso-C_4H_{10} and secondary reactions not included, yields a value of $k_5 = 1.40 \times 10^{-16}$ molecule^{-1} cm^3 s^{-1}. Bottom panel: 19.72 ppmv iso-C_4H_{10} with secondary reactions included (see Table 1), yields a value of $k_5 = 8.21 \times 10^{-17}$ molecule^{-1} cm^3 s^{-1}.

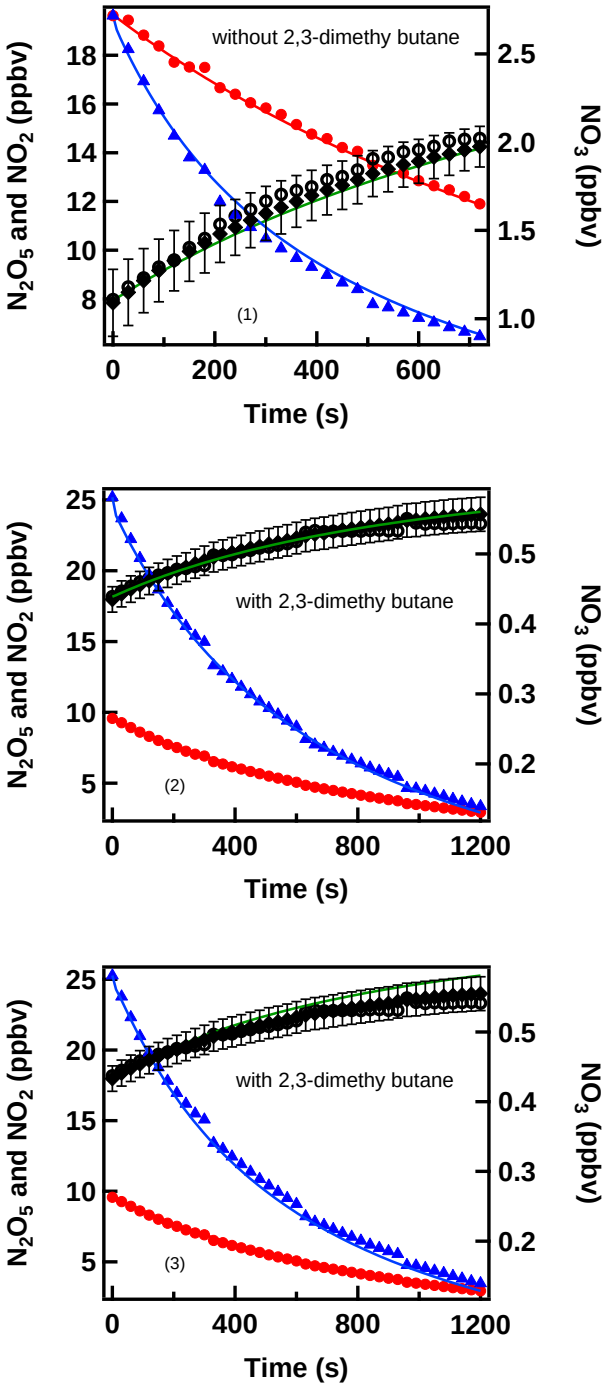

Figure S7. Experimental and simulated NO_3, N_2O_5 and NO_2 concentration profiles versus reaction time. Measured NO_3 (▲), N_2O_5 (●) and NO_2 (◆) are shown along with their simulated temporal profiles (—NO_3, —N_2O_5, —NO_2). Also shown is NO_2 concentration calculated from the Keq and the observed of N_2O_5 and NO_3 concentrations (O). Top panel: 0 ppmv 2,3-dimethy butane. Middle panel: 0.38 ppmv 2,3-dimethy butane and secondary reactions not included, yields a value of $k_6 = 1.25 \times 10^{-15}$ molecule^{-1} cm^3 s^{-1}. Bottom panel: 0.38 ppmv 2,3-dimethy butane with secondary reactions included (see Table 1), yields a value of $k_6 = 6.32 \times 10^{-16}$ molecule^{-1} cm^3 s^{-1}.

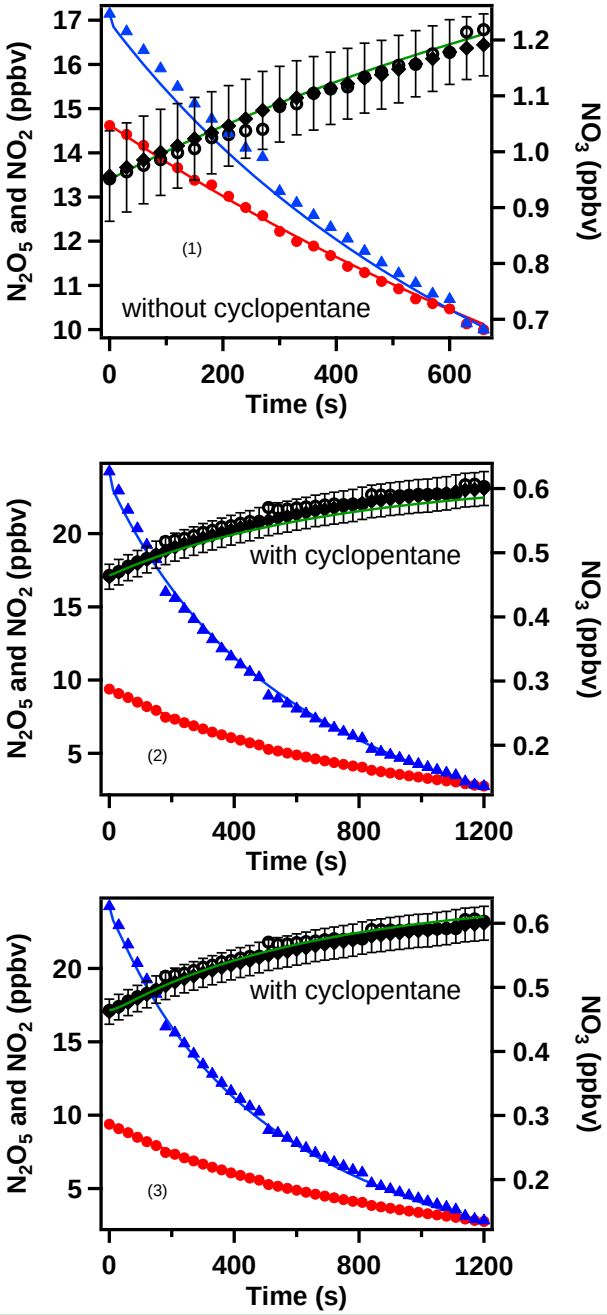

Figure S8. Experimental and simulated NO_3, N_2O_5 and NO_2 concentration profiles versus reaction time. Measured NO_3 (▲), N_2O_5 (●) and NO_2 (◆) are shown along with their simulated temporal profiles (—NO_3, —N_2O_5, —NO_2). Also shown is NO_2 concentration calculated from the Keq and the observed of N_2O_5 and NO_3 concentrations (O). Top panel: 0 ppmv cyclopentane. Middle panel: 0.63 ppmv cyclopentane and secondary reactions not included, yields a value of $k_7 = 2.60 \times 10^{-16}$ molecule^{-1} cm^3 s^{-1}. Bottom panel: 0.63 ppmv cyclopentane with secondary reactions included (see Table 1), yields a value of $k_7 = 1.29 \times 10^{-16}$ molecule^{-1} cm^3 s^{-1}.

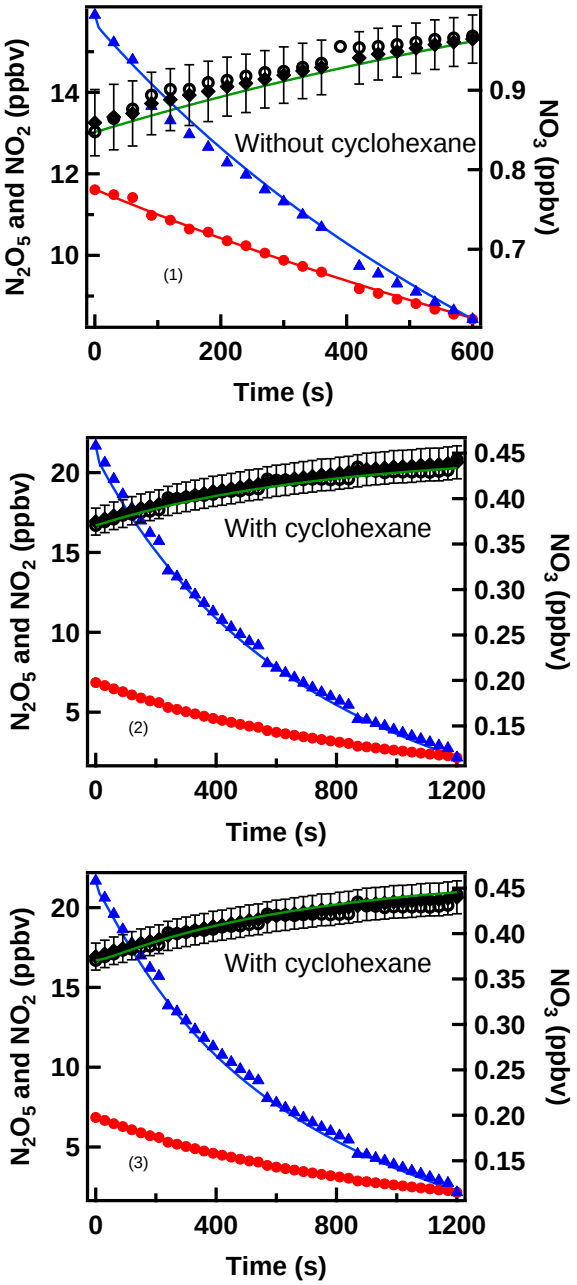

Figure S9. Experimental and simulated NO_3, N_2O_5 and NO_2 concentration profiles versus reaction time. Measured NO_3 (▲), N_2O_5 (●) and NO_2 (◆) are shown along with their simulated temporal profiles (—NO_3, —N_2O_5, —NO_2). Also shown is NO_2 concentration calculated from the Keq and the observed of N_2O_5 and NO_3 concentrations (O). Top panel: 0 ppmv cyclohexane. Middle panel: 1.54 ppmv cyclohexane and secondary reactions not included, yields a value of $k_8 = 2.50 \times 10^{-16}$ molecule^{-1} cm^3 s^{-1}. Bottom panel: 1.54 ppmv cyclohexane with secondary reactions included (see Table 1), yields a value of $k_8 = 1.27 \times 10^{-16}$ molecule^{-1} cm^3 s^{-1}.

Table S1: Reactions of the products of the NO_3 reaction with alkanes and reactive

impurities in the presence of O_2 and nitrogen oxides those were included in simulating the temporal profiles of NO_3 and N_2O_5.

Reaction	Rate coefficients 298 K, 1 bar air (cm^3 $molecule^{-1}s^{-1}$ or s^{-1})	Reference
alkane $+NO_3 \xrightarrow{k_x} R_1 + HNO_3$	k_x (k_1-k_8)	This work
$N_2O_5 \xrightarrow{k_9} NO_3 + NO_2$	0.0369	a
$NO_3 + NO_2 \xrightarrow{k_{10}} N_2O_5$	1.35×10^{-12}	a
$NO_3 \xrightarrow{k_{11}}$ loss	k_{11}	b
$N_2O_5 \xrightarrow{k_{12}}$ loss	k_{12}	b
$R_1 + O_2 \xrightarrow{k_{13}} R_1O_2$	10^{-11}	c
$R_1O_2 + NO_3 \xrightarrow{k_{14}} R_1O + NO_2$		
R_1: CH_3	1.2×10^{-12}	d
R_1: C_2H_5 and other alkyl radical	2.3×10^{-12}	e
$R_1O_2 + R_1O_2 \xrightarrow{k_{15}} 2R_1O$		
R_1: CH_3	3.5×10^{-13}	f
R_1: C_2H_5	7.6×10^{-14}	f
R_1: n-C_3H_7	3×10^{-13}	f
R_1: i-C_3H_7	1×10^{-15}	f
R_1: s-C_4H_9	2.5×10^{-13}	g
R_1: t-C_4H_9	6.7×10^{-15}	g
R_1: cycle-C_6H_5	2.5×10^{-13}	g
$R_1O_2 + NO_2 \xrightarrow{k_{16}} R_1O_2NO_2$		
R_1: CH_3	4.0×10^{-12}	c
R_1: C_2H_5 and other alkyl radical	5.1×10^{-12}	c
$R_1O_2NO_2 \xrightarrow{k_{17}} R_1O_2 + NO_2$		
R_1: CH_3	1.5	c
R_1: C_2H_5 and other alkyl radical	3.4	c
$R_1O + O_2 \xrightarrow{k_{18}} R_2CHO + HO_2$	7.14×10^{-14}	g

$R_1O_2 + HO_2 \xrightarrow{k_{19}} R_1OOH + O_2$		
R_1: CH_3	5.2×10^{-12}	f
R_1: C_2H_5	7.97×10^{-12}	g
R_1: i-C_3H_7	1.19×10^{-11}	g
R_1: s-C_4H_9	1.43×10^{-11}	g
R_1: t-C_4H_9	1.43×10^{-11}	g
R_1: C_6H_{13}	1.76×10^{-11}	g
R_1: cycle-C_6H_{11}	1.76×10^{-11}	g
$R_2CHO + NO_3 \xrightarrow{k_{20}} R_3COOO + HNO_3$		
R_3: H	5.5×10^{-16}	f
R_3: CH_3 and other alkyl radical	2.7×10^{-15}	f
$HO_2 + NO_3 \xrightarrow{k_{21}} OH + NO_2 + O_2$	4×10^{-12}	f
$OH + NO_3 \xrightarrow{k_{22}} HO_2 + NO_2$	2×10^{-11}	f
$NO_2 + OH \xrightarrow{k_{23}} HONO_2$ / HOONO	6.5×10^{-11}	f
alkene $+ NO_3 \xrightarrow{k_{24}} R_4O_2$		
alkene: propene	9.5×10^{-15}	f
$R_4O_2 + NO_3 \xrightarrow{k_{25}} R_4O + NO_2$	2.3×10^{-12}	f
$R_4O_2 + R_1O_2 \xrightarrow{k_{26}} R_4O + R_5OH + R_5CHO$	4.0×10^{-14}	f
$R_4O_2 + R_4O_2 \xrightarrow{k_{27}} R_4O + R_5OH + R_5CHO$	4.0×10^{-14}	f
$R_4O + O_2 \xrightarrow{k_{28}} R_5CHO + HO_2$	7.14×10^{-14}	g

a. J. Burkholder, S. Sander, J. Abbatt, J. Barker, R. Huie, C. Kolb, M. Kurylo, V. Orkin, D. Wilmouth and P. Wine, *Nasa panel for data evaluation technical report*, 2015.

b. (Derived from the first period of the experiments: observation in the absence of alkanes)

c. R. Atkinson, D. L. Baulch, R. A. Cox, J. N. Crowley, R. F. Hampson, R. G. Hynes, M. E. Jenkin, M. J. Rossi and J. Troe, *Atmos. Chem. Phys.*, 2004, **4**, 1461-1738.

d. V. Daele, G. Laverdet, G. Le Bras and G. Poulet, *J. Phys. Chem.*, 1995, **99**, 1470-1477.

e. A. Ray, V. Daële, I. Vassalli, G. Poulet and G. Le Bras, *J. Phys. Chem.*, 1996, **100**, 5737-5744. S. Vaughan, C. E. Canosa-Mas, C. Pfrang, D. E. Shallcross, L. Watson and R. P. Wayne, *Phys Chem Chem Phys*, 2006, **8**, 3749-3760.

f. R. Atkinson, D. L. Baulch, R. A. Cox, J. N. Crowley, R. F. Hampson, R. G. Hynes, M. E. Jenkin, M. J. Rossi, J. Troe and I. Subcommittee, *Atmos Chem Phys*, 2006, **6**, 3625-4055.

g. M. E. Jenkin, S. M. Saunders and M. J. Pilling, *Atmos. Environ.*, 1997, **31**, 81-104.

Table S2 The specification of each alkane

	N_2 (ppmv	O_2 (ppmv	H_2O (ppmv	H_2 (ppmv	CO_2 (ppmv	C_nH_{m*} (ppmv	C_nH_{m**} (ppmv
Methane (≥99.995%)	≤15	≤5	≤5	≤1	≤1	≤20 (C_2H_6≤15)	≤20
Ethane (≥99.995%)	≤15	≤3	≤3	≤5	≤1	≤20 (C_2H_4≤15)	≤20
Propane (≥99.95%)	≤40	≤10	≤5	≤40	≤5	≤200 (C_3H_6≤200)	C_3H_6≤50 C_4H_8≤20
n-butane (≥99.95%)	≤40	≤10	≤5	≤40	≤5	≤400	C_3H_6≤20 C_4H_8≤20
iso-butane (≥99.95%)	≤40	≤10	≤5	≤40	≤5	≤400	C_3H_6≤20 C_4H_8≤20
2,3-dimethy butane (≥99.5%)							≤20
Cyclopentane (≥99%)						Cyclopentene ≤500	≤50
Cyclohexane (≥99.5%)			≤200				≤20

* This is the quoted levels of total hydrocarbon impurities in the sample from the vendor supplied. We assumed that the hydrocarbons could be olefins in assessing some of our measured rate coefficients.

** The impurities in these samples are quantified using a GC-MS, the detection limit of the GC-MS for olefins in alkanes is 20 ppmv.

Table S3. The rate coefficient of NO_3 radical with ethene derived from absolute method by fitting the observed profiles of NO_3 and N_2O_5 to a least squares algorthm.

Compound	Initial mixing ratio of reactants in the chamber				k_{ethene} [a]	k_{ethene} [b] incl. systematic errors
	VOC (ppmv)	NO_3 (ppbv)	N_2O_5 (ppbv)	NO_2 (ppbv)	(cm^3 $molecule^{-1}s^{-1}$)	
ethene	3.48	0.48	16.16	33.79	2.71×10^{-16}	
	6.00	0.59	13.61	23.17	2.26×10^{-16}	
	4.49	0.97	17.76	17.68	2.31×10^{-16}	
				Mean average	$(2.4\pm0.5)\times10^{-16}$	$(2.4\pm0.6)\times10^{-16}$

[a] Quoted error is at the 95% confidence level and is a measure of the precision of our measurements. It includes Student t-distribution contribution due to the limited number of measurements.

[b] The quoted errors include estimated systematic errors as described in the text.